

INVESTIGATIONS OF STGS, SNGS, CTGS, & CNGS MATERIALS FOR USE IN SAW APPLICATIONS

D. Puccio, D. C. Malocha, and Mitch M. C. Chou¹

Center for Applied Acoustoelectronic Technology, School of Electrical Engineering and Computer Science,
University of Central Florida, Orlando, FL 32816-2450

¹Crystal Photonics, Inc., 5525 Benchmark Lane, Sanford, FL 32773

Abstract – Langasite structure compounds have been the focus of much consideration recently, given their higher electromechanical coupling and similar temperature behavior to that of quartz. Recent investigations have begun on four new materials, STGS, SNGS, CTGS, and CNGS. These langasite structure crystals show great promise for use in SAW applications. In some respects, STGS, SNGS, CTGS, and CNGS exhibit better SAW material properties than the LGX materials (langasite, langanite, and langatate) previously studied. For example, SNGS and STGS have higher electromechanical coupling than LGX, in excess of 0.6% and 0.5%, respectively. In addition, all four materials have lower densities resulting in higher phase velocities. Along with previously studied trigonal 32 class materials, there is a good possibility that temperature compensated cuts exist. Recent results are reported for SAW material parameters and device performance at various propagation directions on Y-cut STGS, SNGS, CTGS, and CNGS wafers. These results include coupling coefficient, phase velocity, transducer capacitance, and temperature coefficient of delay (TCD). Experimental measurements of metal strip reflectivity are shown for various metal thicknesses. Measured SAW resonator Q data are also presented. The measurement procedures and the parameter extraction methods for these experiments are discussed. A comparison of the data with previously reported parameters on LGX is presented and a discussion of the results is provided.

I. INTRODUCTION

The purpose of this work is to investigate and extract basic SAW material parameters and present SAW resonator performance. Electromechanical coupling, phase velocity, and transducer capacitance will be presented as a function of propagation for Y-cut wafers of STGS, SNGS, CTGS, and CNGS. In addition, reflectivity per wavelength will be presented as a function of normalized metal thickness for YX propagation on each substrate. These results will be compared with previously published results for LGX materials (langatate, langasite, and langanite) and quartz [1,2]. Finally, recently obtained two-port SAW resonator results will be presented.

II. EXPERIMENTAL CONDITIONS

All devices were tested using an RF probe station, which allows for devices to be tested directly on the wafer. A computer-controlled HP 8753C Automatic Network

Analyzer was used to obtain the data. The probe station and ANA were calibrated using a Cascade Microtech calibration wafer. Temperature coefficient of frequency (TCF) measurements were made over a range of 10°C to 200°C using a temperature controlled chuck.

III. DELAY LINE MEASUREMENTS

A. Delay line device parameters

Each material's coupling coefficient, phase velocity, and transducer capacitance was extracted from simple delay line measurements [3]. The delay lines used had center frequency wavelengths of 32 μm . Each transducer was 20 wavelengths long and the separation between transducers was 25 wavelengths. The delay lines were fabricated using a thin film titanium layer followed by aluminum. Aluminum thickness was typically around 2000Å.

B. Parameter extraction method

The measured S_{21} data was used to extract center frequency. The data was first converted to the time domain using an FFT. Next, spurious time responses were removed and the data converted back to the frequency domain. The extraction of center frequency was accomplished by minimizing the error between the measured data and the theoretical predictions over the delay line pass band. The solution obtained for center frequency was then used in further optimizations. No compensation was made for metallization effects on the center frequency.

Next, the S_{11} data was converted to Z_{11} where the parasitic resistance was removed. Z_{11} is then converted to Y_{11} where the real part is the acoustic conductance. Using the center frequency obtained previously, a minimization of the error between the measured and predicted conductance yields the center frequency acoustic conductance.

The transducer static capacitance is obtained by performing a linear regression fit to the imaginary part of Y_{11} . The frequency range for this optimization was greater than three null bandwidths. This condition is required for an accurate solution due to the effect of the acoustic susceptibility in the delay line pass band.

Using the center frequency, acoustic conductance, mark-to-pitch ratio, and static capacitance, the electrostatic field solutions for transducer admittance given by Morgan

The authors acknowledge support under contracts from the Army Research Office #DAAD19-02-1-0440, and Crystal Photonics.

TABLE I
VELOCITY, COUPLING AND CAPACITANCE RESULTS

Material	Angle (around X)	Velocity (m/sec)	Coupling Coefficient	Cs (pF/cm)
SNGS Y	0°	2835.8	0.628%	1.30
SNGS Y	15°	2863.6	0.506%	1.34
SNGS Y	30°	2925.3	0.344%	1.35
SNGS Y	45°	2992.9	0.179%	1.51
SNGS Y	60°	3063.9	0.085%	1.57
SNGS Y	75°	3119.9	0.048%	1.70
STGS Y	0°	2733.1	0.562%	1.24
STGS Y	30°	2818.4	0.308%	1.23
STGS Y	45°	2889.2	0.167%	1.51
STGS Y	60°	2954.8	0.090%	1.52
STGS Y	75°	3011.2	0.032%	1.60
CTGS Y	0°	2771.6	0.326%	1.75
CTGS Y	15°	2780.8	0.250%	1.77
CTGS Y	30°	2800.3	0.170%	1.75
CTGS Y	45°	2824.3	0.101%	1.78
CTGS Y	60°	2850.9	0.051%	1.83
CNGS Y	0°	2906.2	0.261%	1.81
CNGS Y	15°	2910.8	0.218%	1.55
CNGS Y	30°	2927.6	0.135%	1.61
CNGS Y	45°	2943.5	0.089%	1.84
CNGS Y	60°	2960.9	0.042%	2.03
LGT Y	2°	2210.6	0.423%	2.08
LGT Y	15°	2290.7	0.360%	2.30
LGT Y	30°	2341.4	0.187%	2.30
LGT Y	45°	2345.1	0.079%	2.50
LGT Y	60°	2436.0	0.036%	3.34
LGT Y	75°	2596.7	0.019%	3.43

were used to determine the electromechanical coupling coefficient [4].

C. Results

Table 1 shows a summary of current results for phase velocity, electromechanical coupling, and transducer capacitance for STGS, SNGS, CTGS, and CNGS at various propagation angles. In addition, previously published results for LGT Y-cut substrates are also presented for comparison [5]. The coupling coefficients for STGS and SNGS are shown to be higher than that of LGT, while CTGS and CNGS are lower. However, all four materials are shown to have at least 20% higher phase velocities than LGT. These results are in good agreement with those published in [6].

IV. TEMPERATURE COEFFICIENT MEASUREMENTS

TCF measurements were made using two-port resonators. The peak S-parameter response was tracked as the temperature ranged from 10°C to 200°C. From these measurements, the fractional frequency changes and temperature coefficients were obtained.

Fig. 2 shows a typical fractional frequency plot for CNGS 45° rotated around X. The results for STGS, SNGS, CTGS, and CNGS are summarized in Table 2. Previously published LGT Y-cut TCF measurements are also shown for comparison [5]. The most notable results from these measurements are the presence of temperature compensated cuts on CTGS and CNGS at approximately 40° and 45° rotated from X, respectively. It is also interesting to note the range of TCF values for these five langasite-structure compounds. SNGS and STGS have relatively high negative TCF values of approximately -90 ppm/°C which implies turnover temperatures well below 0°C. However, CTGS and CNGS have temperature coefficients centered on zero indicating turnover temperatures near room temperature. Finally, LGT-Y has been shown to have temperature coefficients of approximately +50 ppm/°C signifying turnover temperatures much greater than room temperature. This wide range of temperature behavior is indicative of the potential of langasite-structure compounds in various SAW applications for frequency control and sensors.

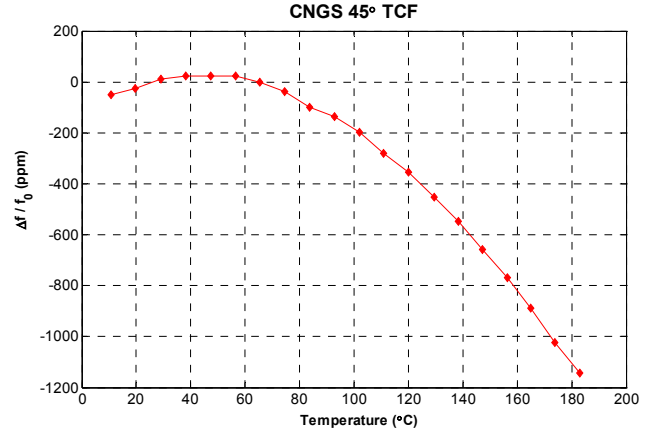


Fig. 1 Typical fractional frequency plot for CNGS 45° rotated from X

V. REFLECTIVITY MEASUREMENTS

A. Reflectivity device parameters

SAW reflectivity was obtained using a test mask with devices having various center frequency wavelengths. The center frequency wavelength varied from 18 to 80 μm . Each test structure was a simple delay line with a reflector grating situated nearby [1,7]. The transducers were 20 wavelengths long and separated by 25 wavelengths. The reflector grating contained 100 electrodes and was situated 50 wavelengths away from the delay line. The devices were fabricated using a thin film titanium layer followed by aluminum.

B. Reflectivity extraction method

SAW Reflectivity was obtained for YX propagation (Euler angles $[0^\circ \ 90^\circ \ 0^\circ]$) on STGS, SNGS, CTGS, and CNGS wafers. Multiple wafers were fabricated and tested using the test mask described. S-parameter

measurements were taken over the pass bands of the devices described. S_{21} responses were converted to the time domain using an FFT. The delay line and reflector responses were then gated individually in the time domain and converted back to the frequency domain. The reflector response was then normalized by the delay line response, thereby eliminating the delay line's effect on the reflector response. Using the electromechanical coupling obtained previously in conjunction with the metallization ratio (h/λ), a coupling-of-modes model was used to predict an ideal reflector response [8]. A minimization of the error between the measured and predicted reflector responses was performed, where reflectivity per wavelength was used as a variable.

TABLE II
TCF RESULTS FOR STGS, SNGS, CTGS, CNGS,
AND LGT Y-CUT WAFERS

Material	Angle (around X)	TCF
STGS Y	0°	-73.1
STGS Y	15°	-70.7
STGS Y	30°	-65.0
STGS Y	45°	-60.5
STGS Y	60°	-56.5
SNGS Y	0°	-98.9
SNGS Y	15°	-93.0
SNGS Y	30°	-84.3
SNGS Y	45°	-80.7
SNGS Y	60°	-71.9
CTGS Y	0°	-37.1
CTGS Y	15°	-31.8
CTGS Y	30°	-20.3
CTGS Y	45°	7.9
CTGS Y	60°	44.0
CTGS Y	75°	70.5
CNGS Y	0°	-52.0
CNGS Y	15°	-43.6
CNGS Y	30°	-26.5
CNGS Y	45°	1.4
CNGS Y	60°	37.5
LGT Y	2°	64.5
LGT Y	21°	42.4
LGT Y	30°	46.3
LGT Y	45°	61.4
LGT Y	62°	53.9
LGT Y	74°	24.6

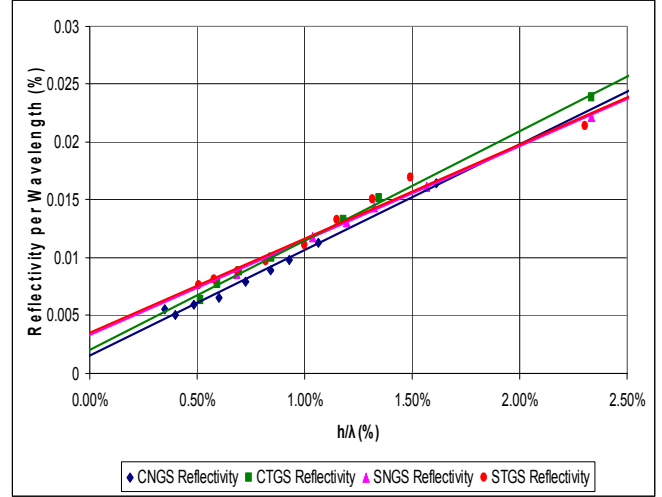


Fig. 2 Reflectivity per wavelength results for YX propagation on STGS, SNGS, CTGS, and CNGS

Results for STGS, SNGS, CTGS, and CNGS YX reflectivity are shown in Fig. 2. The results are shown to be very similar for all four materials. For YX propagation, each material has maximum coupling in the plane. However, TCF measurements are shown to be between -30 and -100 ppm/°C. SNGS and STGS have nearly identical slopes, which indicate very similar mass loading contributions to reflectivity. The same is true for CNGS and CTGS. However, SNGS and STGS have slightly higher mass loading contributions than CNGS and CTGS. Compared to ST quartz, the reflectivity per wavelength is similar [2]. These results also agree well with [6]. When compared with LGX, the reflectivity is shown to be more than twice of LGT and LGN XY and YX propagations. However, the results are very similar to those found for LGT and LGN 30° rotated from X propagation [1]. The y-intercept of each line is an indicator of the piezoelectric shorting effect alone. Therefore, using known equations, and estimate of the coupling coefficient can be obtained. The estimated coupling coefficients are 0.47%, 0.44%, 0.27%, 0.2% for STGS, SNGS, CTGS, and CNGS, respectively. These values are all slightly less than those extracted using the previous techniques, which is believed to be more accurate.

VI. RESONATOR RESULTS

Several two-port resonators were fabricated and tested for temperature coefficient extraction. In addition, two-port resonator Q values were obtained from these data. Table 3 contains Q's for resonators at various propagation angles on STGS, SNGS, CTGS, and CNGS. The best extracted data showed a Q in excess of 4700. Shown in Fig. 3 is a typical two-port resonator response. This device was fabricated and tested on STGS at 15° rotated from X. This particular device exhibited a Q of approximately 2500.

TABLE III.
RESONATOR RESULTS FOR VARIOUS ORIENTATIONS
ON STGS, SNGS, CTGS, AND CNGS

Material	Angle (around X)	Q
STGS	15°	2571
SNGS	45°	3912
CTGS	45°	4715
CNGS	15°	3254

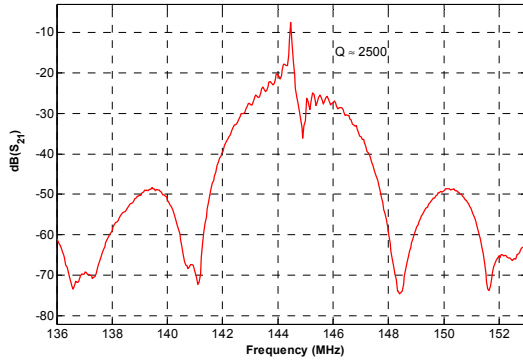


Fig. 3 Typical two-port resonator response for
STGS 15° rotated from X

All of the two-port resonators tested had metallization ratios, h/λ , approximately equal to 1%.

VII. CONCLUSION

SAW material parameters have been extracted for Y-cut STGS, SNGS, CTGS, and CNGS at various propagation angles. Electromechanical coupling values show similar results to those of LGX. However, the phase velocities of STGS, SNGS, CTGS, and CNGS are more than 20% higher than those previously published for LGX. TCF measurements have been made for various propagation angles and show promising results. Most notably, CTGS and CNGS have been shown to have temperature compensated cuts at 40° and 45° rotated from X, respectively. In addition, the wide range of temperature behaviors for langasite-structure compounds has been discussed. Initial two-port resonator results and Q values have been given.

These materials exhibit very promising SAW properties and additional work is required to fully explore their potential for resonant devices, filters, and sensors. The material has higher coupling than quartz on many cut angles, it has been demonstrated to be stable at high temperatures, the various materials have a range of TCFs which may be useful in frequency control and sensors, and work is required to study acceleration affects for vibration and shock environments. The rather large number of materials in this langasite-family-structure provides the

possibility of “designer-materials” for device applications. Much work is needed to perfect the growth of these materials as well as their characterization. Currently, the limited amount of materials available is dictating the exploration of these new materials for possible device use.

ACKNOWLEDGMENTS

The authors are grateful for support and discussions from Drs. Shen Jen and Bruce Chai of Crystal Photonics, Inc. The authors are grateful to M.P. da Cunha from the University of Maine for many helpful discussions on materials.

REFERENCES

- [1] D. Puccio, N. Saldanha, D. C. Malocha, and M.P. da Cunha, “SAW Reflectivity and Resonator Results for LGT and LGN”, 2001 IEEE International Frequency Control Symposium Proceedings, pp. 324-327.
- [2] Supriyo Datta, *Surface Acoustic Wave Devices*, Prentice Hall, N.J., 1986, Chapter 6.
- [3] D.C. Malocha, M.P. da Cunha, E.L. Adler, D. Puccio and K. Knapp, “Measurements and Predictions of SAW Parameters and Device Performance on LGT-X Substrates”, 2001 IEEE International Frequency Control Symposium Proceedings, pp. 219-222.
- [4] D.P. Morgan, *Surface Wave Devices for Signal Processing*, Elsevier, N.Y., 1991, Chapter 4
- [5] D.C. Malocha, M.P. da Cunha, D. Puccio and K. Casey, “Investigations of Langanite and Langatate Materials for use in SAW Device Applications”, 2001 IEEE International Ultrasonics Symposium Proceedings, pp. 231-234.
- [6] M.M.C. Chou, S. Jen, B.H.T. Chai, “Investigation of Crystal Growth and Material Constants of Ordered Langasite Structure Compounds”, 2001 IEEE International Frequency Control Symposium Proceedings, pp. 250-254.
- [7] P.V. Wright, “Modeling and Experimental Measurements of the Reflection Properties of SAW Metallic Gratings”, 1984 IEEE International Ultrasonics Symposium Proceedings, pp. 54-63.
- [8] Dong-Pei Chen and H. Haus, “Analysis of Metal-Strip SAW Gratings and Transducers”, IEEE Transactions on Sonics and Ultrasonics, Vol. SU-32, No. 3, May 1985.